

Comparative Study of Different Methods for the Prediction of Drug–Polymer Solubility

Matthias Manne Knopp^{†‡}, Lidia Tajber[§], Yiwei Tian^{||}, Niels Erik Olesen^{†,⊥}, David S. Jones^{||}, Agnieszka Kozyra[§], Korbinian Löbmann[#], Krzysztof Paluch[§], Claire Marie Brennan[§], René Holm^{*†}, Anne Marie Healy[§], Gavin P. Andrews^{||}, and Thomas Rades[#]

[†] Department of Biologics and Pharmaceutical Science, H. Lundbeck A/S, 2500 Valby, Denmark

[‡] School of Pharmacy, Johannes Gutenberg University Mainz, 55099 Mainz, Germany

[§] School of Pharmacy and Pharmaceutical Sciences, Trinity College Dublin, Dublin 2, Ireland

^{||} Pharmaceutical Engineering Group, School of Pharmacy, Medical Biology Centre, Queen's University, Belfast BT9, Northern Ireland

[⊥] NSM, Research Unit for Functional Biomaterials, Roskilde University, 4000 Roskilde, Denmark

[#] Department of Pharmacy, University of Copenhagen, 2100 Copenhagen, Denmark

*Tel: +45-3643-3596. Fax: +45-3643-2131. E-mail: rhol@lundbeck.com

Abstract

In this study, a comparison of different methods to predict drug–polymer solubility was carried out on binary systems consisting of five model drugs (paracetamol, chloramphenicol, celecoxib, indomethacin, and felodipine) and polyvinylpyrrolidone/vinyl acetate copolymers (PVP/VA) of different monomer weight ratios. The drug–polymer solubility at 25 °C was predicted using the Flory–Huggins model, from data obtained at elevated temperature using thermal analysis methods based on the recrystallization of a supersaturated amorphous solid dispersion and two variations of the melting point depression method. These predictions were compared with the solubility in the low molecular weight liquid analogues of the PVP/VA copolymer (N-vinylpyrrolidone and vinyl acetate). The predicted solubilities at 25 °C varied considerably depending on the method used. However, the three thermal analysis methods ranked the predicted solubilities in the same order, except for the felodipine–PVP system. Furthermore, the magnitude of the predicted solubilities from the recrystallization method and melting point depression method correlated well with the estimates based on the solubility in the liquid analogues, which suggests that this method can be used as an initial screening tool if a liquid analogue is available. The learnings of this important comparative study provided general guidance for the selection of the most suitable method(s) for the screening of drug–polymer solubility.

Keywords:

amorphous; calorimetry (DSC); Flory–Huggins; melting point depression; polymers; recrystallization; solid dispersion; solubility; thermal analysis; thermodynamics

Introduction

The development of amorphous drug formulations has attracted a lot of attention, both in the pharmaceutical industry and in academic research, owing to the potential enhancement of solubility and dissolution rate of poorly water-soluble drug candidates.(1-3) However, the number of formulations containing drug in the amorphous form that have made it through to the market is limited due to the generally poor physical stability of the amorphous form.(4-6) The high internal free energy of amorphous compounds often results in fast recrystallization with the subsequent loss of the dissolution rate and solubility advantages.(7) Therefore, a key requirement for any amorphous formulation to succeed is that it be stable against crystallization during the shelf life of the formulation.

Incorporation of the amorphous drug into a polymer with a higher glass transition temperature (T_g) will generally increase the T_g of the resulting mixture, reducing the molecular mobility and thus nucleation and crystal growth of the drug and therefore improving the kinetic stability.(8) This is commonly known as an amorphous solid dispersion and can be defined as a molecular dispersion of the drug in an amorphous polymer matrix. Even though this is a promising approach, it does not ensure physical stability during storage, as the drug can still crystallize at temperatures well below the T_g .(9) Consequently, in order to stabilize the system thermodynamically it is essential that the drug be molecularly dispersed in the polymer below its saturation solubility, and therefore, determination of drug–polymer solubility is of great importance for the rational development of amorphous systems.(2, 10) However, as the majority of pharmaceutically relevant drugs and polymers are solid (or highly viscous) at ambient temperature, measuring the drug–polymer solubility constitutes a major challenge.(11) Therefore, several differential scanning calorimetry (DSC) protocols have been proposed based on determination of equilibrium thermodynamics at elevated temperature and extrapolation to room temperature.(11-15)

The initial protocols exploited the melting point depression of a drug in the presence of a polymer.(12, 16, 17) The concept of melting point depression to describe the interaction between a crystalline polymer and an amorphous polymer can be derived from the Flory–Huggins expression of chemical potential of mixing and the condition of phase equilibrium.(18, 19) In theory, melting of a crystal occurs at the temperature when the chemical potential of the crystal is equal to the chemical potential of the melt. Addition of an amorphous polymer to the crystal may (if miscible) reduce the chemical potential of the crystalline material, leading to melting point depression.(18, 19) Consequently, by extending the equations presented by Flory–Huggins to fit crystalline drug–polymer systems and assuming that amorphous drug behaves as a solvent, it is possible to relate the solubility of a drug in a polymer to the melting point depression of the drug.(12, 20)

In a protocol developed by Marsac et al.(12) physical drug–polymer mixtures of known composition were prepared by geometric mixing and analyzed by DSC. The onset of the bulk melting endotherm (T_m) was considered the equilibrium solubility temperature of the given composition. The onset of the melting was chosen to eliminate the impact of sample preparation on the T_m .(21, 22) This protocol was further developed by Tao et al.,(11) who introduced cryomilling of the physical mixtures before DSC analysis in order to compensate for the slow dissolution kinetics by reducing particle size to allow for diffusive mixing.(7) In this case the end point of the dissolution endotherm (T_{end}) was considered the equilibrium solubility temperature of the given composition. The end point (offset) value was chosen because this value represents the melting point of the final composition, assuming complete mixing has occurred.(11, 13, 23) This approach is currently the most commonly used in the literature to determine drug–polymer solubility.(10, 11, 13, 24-27)

As a result of the high viscosity of polymers, the dissolution kinetics are slow and can potentially (depending on heating rate) exceed the time scale of the DSC scan.(11) This may result in a higher dissolution end point and ultimately lead to an underestimation of the drug–polymer solubility.(7) Therefore, Mahieu et al.(14) proposed a protocol that takes advantage of the fact that recrystallization is generally faster than dissolution. In this method, a supersaturated amorphous solid dispersion was annealed at different temperatures above the recrystallization temperature until the equilibrium solubility was reached.(14, 28, 29) The equilibrium solubility concentration was then derived directly from the T_g of the annealed material using the Gordon–Taylor relationship.(30)

Even though they vary in detail, the different approaches used to determine the drug–polymer solubility reported in the literature can be divided into three general thermal analysis methods: (i) the recrystallization method,(14) (ii) the dissolution end point method,(10, 11) and (iii) the melting point depression method.(12) Despite the increased interest in determination of drug solubility in polymers, to the best of our knowledge, no comparative study across methods has been conducted. The aim of this study was therefore to compare the three aforementioned thermal analysis methods, through formal statistical analysis, for the prediction of drug–polymer solubility using binary systems consisting of five model drugs (paracetamol, chloramphenicol, celecoxib, indomethacin, and felodipine) and polyvinylpyrrolidone/vinyl acetate copolymers (PVP/VA) of different vinylpyrrolidone/vinyl acetate weight ratios (30/70, 50/50, 60/40, 70/30, and 100/0). The model drugs were selected in order to cover a range of general physicochemical properties of low molecular weight drugs; i.e., T_m (140–175 °C), T_g (20–60 °C), and molecular weight (M_w , 150–400 g/mol).

In addition to the three thermal analysis methods described above, it is possible to estimate the solubility of a drug in a polymer from the solubility of the drug in a liquid low molecular weight

analogue of the polymer using the Flory–Huggins lattice model.(13, 25) Therefore, drug–polymer solubilities obtained using the three thermal analysis methods were compared with a prediction based on the solubility of the drugs in the liquid monomeric precursors to the copolymer (*N*-vinylpyrrolidone and vinylacetate). The ultimate aim of this comparative study was to provide a general guidance for the screening of polymers suitable for glass solutions.

Experimental Section

Materials

Paracetamol (PCM, $M_w = 151.17$ g/mol) and chloramphenicol (CAP, $M_w = 323.13$ g/mol) were purchased from Sigma-Aldrich Co. (St. Louis, MO, USA). Celecoxib (CCX, $M_w = 381.37$ g/mol) was purchased from AK Scientific, Inc. (Union City, CA, USA). Indomethacin (IMC, $M_w = 357.79$ g/mol) was purchased from Hawkins Pharmaceutical Group (Minneapolis, MN, USA). Felodipine (FDP, $M_w = 384.26$ g/mol) was purchased from Combi-Blocks, Inc. (San Diego, CA, USA). *N*-Vinylpyrrolidone (NVP, $M_w = 111.14$ g/mol) and vinyl acetate (VA, $M_w = 86.09$ g/mol) were purchased from Sigma-Aldrich Co. (St. Louis, MO, USA). Plasone K-17 (PVP K17, $M_w = 10000$ g/mol), PVP/VA copolymer E-335 (PVP/VA 335, $M_w = 28000$ g/mol), PVP/VA copolymer E-535 (PVP/VA 535, $M_w = 36700$ g/mol), PVP/VA copolymer E-635 (PVP/VA 635, $M_w = 38200$ g/mol), and PVP/VA copolymer E-735 (PVP/VA 735, $M_w = 56700$ g/mol) were kindly supplied by Ashland Chemical Co. (Columbus, OH, USA). Since the PVP/VA copolymers were sourced as solutions, they were converted to the solid forms by spray drying. The supplied liquids were diluted with ethanol to form 5% (w/w) solutions and processed, using the Mini Spray Dryer B-290 from Büchi (Flawil, Switzerland) in the open pressure mode with air as drying gas, applying the following conditions: inlet temperature 140 °C, aspirator rate 100%, and pump speed 30%. These parameters resulted in an outlet temperature of around 80 °C.

Liquid Analogue Solubility Approach

Solubility Measurements

The solubility of the different drugs in the liquid analogues NVP and VA was determined using the shake-flask method. An excess of crystalline drug was added to a capped glass tube containing 1 mL of the liquid analogue and shaken for 72 h using a mechanical rotor from Heto Lab Equipment (Birkerød, Denmark). Samples were withdrawn, filtered using a 0.2 µm PTFE hydrophobic syringe filter from Merck Millipore Ltd. (Darmstadt, Germany), and diluted with mobile phase to appropriate concentrations. The diluted samples were assayed using a HPLC system composed of an L-7100 pump, an L-7200 auto sampler, a T-6000 column oven, and a D-7000 interface, all from Merck-Hitachi LaChrom (Tokyo, Japan). A reverse phase X-Bridge C-18 column (4.6 × 150 mm, 3.5 µm) from Waters

(Milford, MA, USA) was used for the separation, and the mobile phase consisted of methanol and 0.0025 M potassium dihydrogen phosphate aqueous buffer (72:28 v/v) adjusted to pH 3 with phosphoric acid. A variable wavelength ultraviolet L-7450A diode array detector from Merck-Hitachi LaChrom (Tokyo, Japan) was used to detect signals at wavelengths 280, 280, 250, 270, and 230 nm and retention times 1.62, 2.03, 8.06, 4.04, and 11.95 min for PCM, CAP, CCX, IMC, and FDP, respectively.

Recrystallization Method

Sample Preparation

Supersaturated amorphous solid dispersions were prepared by a film casting method. The drug and polymer (80:20 or 85:15 w/w, 500 mg) were dissolved in 5 mL of acetone:ethanol (80:20 v/v) and cast onto a Teflon coated 76 × 26 mm Menzel glass. The solvent was evaporated on a Jenway 1100 hot plate from Bibby Scientific Ltd. (Staffordshire, U.K.) using a plate temperature of 150 °C. The dried samples were scraped of the Teflon coated glass plate and gently ground using a mortar and pestle.

Thermal Analysis

The cast film powders and pure compounds were analyzed using a Q2000 DSC from TA Instruments Inc. (New Castle, DE, USA). Sample powders (2–3 mg) were scanned under 50 mL/min pure nitrogen gas purge using Tzero aluminum hermetic pans with a perforated lid. The temperature and enthalpy of the DSC instrument were calibrated using indium. The melting temperature (T_m , onset), melting enthalpy (ΔH_m), glass transition temperature (T_g , inflection), and heat capacity change (ΔC_p) were determined using the Universal Analysis 2000 (version 4.5A) software.

Solubility Determination

The supersaturated amorphous solid dispersions were loaded into the DSC and annealed at different temperatures below the T_m of the particular drug under investigation for 3 h to crystallize the excess drug in the mixture and to reach equilibrium solubility. After annealing, the sample was cooled to -10 °C and ramped at a rate of 5 °C/min to determine the T_g of the annealed material. The concentration of drug remaining in the polymer matrix was then derived directly from the T_g of the annealed material. In order to determine the composition dependence of the T_g , **physical mixtures of drug–polymer of known composition were prepared using a mortar and pestle.** The samples were then heated above the T_m of the pure drug, quench cooled to -10 °C *in situ* in the DSC, and ramped at a rate of 5 °C/min to determine the T_g . For a detailed description of the method, please refer to Mahieu et al.(14) and Knopp et al.(28)

Solid State Characterization

X-ray powder diffraction (XRPD) analysis was performed using an X'Pert PRO MRD diffractometer from PANalytical (Almelo, The Netherlands) equipped with a TCU 100 temperature control unit and an X'Celerator detector using nickel-filtered Cu K α radiation ($\lambda = 1.5406 \text{ \AA}$) at 45 kV and 40 mA. Approximately 1 mg of sample powder was placed on zero background Si plates and measured over the angular range 3–40° 2 θ at a scan rate of 1.20° 2 θ /min. The diffractograms were analyzed using the X'Pert Data Viewer (version 1.2) software.

Dissolution End Point Method

Sample Preparation

Drug and polymer mixtures with different compositions were first mixed using a mortar and pestle followed by mixing in a MM 200 ball mill mixer from Retsch GmbH (Haan, Germany). The individual materials were kept in a drying chamber for at least 24 h at 50 °C before sample preparation. In a typical milling procedure, pure drug or drug–polymer powder samples of 500 mg were loaded in 25 mL stainless steel milling containers with two stainless steel balls (15 mm in diameter) and milled at 20 Hz. A predefined milling time of 2 min was chosen, which was subsequently followed by a 2 min cooling time. The number of milling–cooling cycles to be used for each drug–polymer combination was determined by measuring the melting end point of the mixture, where no further decrease in the melting end point was observed with increased number of milling–cooling cycles. Longer milling time enhanced the dissolution rate of the crystalline drug into the polymer but decreased the sensitivity of the DSC measurement due to increased amorphous content (observed by XRPD). Thus, fewer milling–cooling cycles were used for mixtures containing lower drug loadings.

Thermal Analysis

Samples were analyzed using the power compensation DSC8000 from PerkinElmer (Waltham, MA, USA). Nitrogen was used as the purge gas for low speed scanning. Approximately 8–10 mg of freshly ball-milled sample was packed into an aluminum pan with a perforated lid. Melting point end point determination was conducted at a heating rate of 1 °C/min from 20 to 200 °C. The end point of the melting endotherm (T_{end}) was calculated from the intercept point of the endothermic trace and the postmelting baseline.

Solid State Characterization

The solid state properties of the ball-milled samples were determined using a MiniFlex II X-ray powder diffractometer from Rigaku Corp. (Tokyo, Japan). Radiation was generated from a copper source

operating at a voltage of 30 kV and a current of 15 mA. The test samples were packed into a glass sample holder and scanned from 0 to 40° 2 θ , using a step width of 0.01° 2 θ and a scan rate of 1° 2 θ /min; continuous mode was used. There were certain levels of increased amorphous halo background in the XRPD pattern of ball-milled samples in comparison to crystalline drug and amorphous polymer physical mixtures, but the polymorphic form of all crystalline drugs was determined to be the same as that of the starting drug materials.

Melting Point Depression Method

Sample Preparation

Physical mixtures (w/w) of drug and polymer were prepared by ball milling at 400 rpm for 10 min with a PM 100 planetary ball mill from Retsch GmbH (Haan, Germany) at room temperature. A total amount of 500 mg was loaded to the stainless steel milling container with a volume of 25 mL, and two stainless steel balls (15 mm in diameter) were used. Care was taken to ensure that no polymorphic transition occurred and crystalline API was still present at the end of milling (confirmed by XRPD).⁽²⁶⁾ Collected samples were stored in a desiccator over silica gel at 5 °C until use.

Thermal Analysis

The melting events of the physical mixtures were measured using a Diamond DSC from PerkinElmer (Waltham, MA, USA) with HyperDSC and a ULSP-130 cooling system from ULSP BV (Ede, The Netherlands) operated under a nitrogen flow of 40 mL/min. The gas flow was controlled using a Thermal Analysis Gas Station (TAGS) from PerkinElmer (Waltham, MA, USA). The instrument was calibrated for both melting onset and enthalpy with indium. Before the measurement, samples (5–8 mg) in standard aluminum DSC pans were first annealed for 2 h in an oven from Memmert GmbH (Schwabach, Germany) at a temperature 10 °C above the glass transition temperature of the polymer. The 2 h annealing time was chosen based on a comparison of the heat of fusion values obtained for the 90:10 w/w drug–polymer physical mixtures of nonannealed sample and samples annealed for 2, 4, and 6 h. Samples were then cooled down to room temperature, and the final sample weight was determined. The DSC program used was as follows: samples were first heated to 100–120 °C at a heating rate of 10 °C/min, and then a heating rate of 1 °C/min was applied to obtain the melting temperature value as close to the equilibrium as possible. All curves were evaluated, and the values of melting point (T_m , onset) and melting enthalpies (ΔH_m) were determined. In order to determine the T_g of the drug–polymer mixtures, the samples were preheated in the DSC pans from 100 °C to a temperature above the T_m of drug at a 10 °C/min heating rate and then cooled to 30–40 °C below the expected T_g at a cooling rate of 300 °C/min, and then a step scan method was applied to determine

the T_g . For the step scan, the samples were heated to 30–40 °C above the expected T_g at 5 °C/min in 2 °C steps. A 1 min isothermal step was applied between each of the dynamic steps.

Solid State Characterization

XRPD analysis on all physical mixtures was conducted using a Rigaku MiniflexII Desktop X-ray diffractometer (Tokyo, Japan) with a Haskris cooling unit (Grove Village, IL, USA). The tube output voltage used was 30 kV, and tube output current was 15 mA. A Cu tube with Ni filter suppressing K β radiation was used. Measurements were taken from 5 to 40° 2 θ at a scan rate of 0.05° 2 θ /s. A zero background Si plate was used during measurements to support the sample.

Density Determination

The amorphous densities of the materials were determined using an AccuPyc 1330 helium pycnometer from Micromeritics Instruments Corp. (Norcross, GA, USA). Prior to the measurements, approximately 1 g of the samples was melt quenched to remove any sorbed moisture and to obtain the amorphous form. The samples were weighed before analysis and purged with 19.5 psig dry helium. The reported results are averages of 10 consecutive measurements.

Theoretical Considerations

Prediction of Drug–Polymer Solubility from Drug–Analogue Solubility

Considering that a low molecular weight liquid analogue constitutes the lattice of a polymer, the molecular volume, activity coefficient, and experimental solubility in the analogue can be used to estimate the solubility of the drug in the polymer.⁽²⁵⁾ The activity coefficient in an analogue (γ_{analogue}) is the ratio of ideal mole fraction solubility (X_{id}) and the experimental mole fraction solubility of drug in the analogue (X_{drug}). The X_{drug} in the analogue is obtained experimentally from HPLC analysis as described above, and X_{id} is calculated using⁽²⁵⁾

$$\ln(X_{\text{id}}) = -\frac{\Delta H_m(T_m - T)}{R(T_m T)} + \frac{\Delta C_p(T_m - T)}{RT} - \frac{\Delta C_p}{R} \ln\left(\frac{T_m}{T}\right) \quad (1)$$

where ΔH_m and T_m are the enthalpy of fusion and melting temperature for the drug, respectively, ΔC_p is the heat capacity change at the glass transition of the amorphous drug, R is the gas constant, and T is the temperature for which the solubility estimate is desired. The γ_{analogue} can now be used to calculate the activity coefficient in the polymer (γ_{polymer}) at the solubility limit using⁽¹³⁾

$$\ln(\gamma_{\text{polymer}}) = \ln(\gamma_{\text{analogue}}) + \frac{MV_{\text{drug}}}{MV_{\text{analogue}}} \left[\frac{1}{m_{\text{drug}}} \ln\left(\frac{v_{\text{drug}}}{X_{\text{drug}}}\right) + \frac{1}{m_{\text{drug}}} - \frac{1}{m_{\text{polymer}}} v_{\text{polymer}} \right] \quad (2)$$

where MV_{drug} and MV_{analogue} are the molar volume of drug and analogue, respectively, m_{drug} and m_{polymer} are the ratio of the volume of drug and polymer to the analogue, respectively, and v_{drug} and v_{polymer} are the volume fraction of drug and polymer, respectively. Finally, the mole fraction solubility of crystalline drug in the polymer can be derived from the ratio of X_{id} to v_{polymer} and converted to mass fraction (w/w) for comparison with the experimentally determined solubility.

Prediction of Drug–Polymer Solubility from DSC Data

The experimental solubility of drug in the polymer at elevated temperature was determined using the analytical protocols described in the Experimental Section. The data sets were fitted with the Flory–Huggins model in order to predict the solubility at ambient temperature by extrapolation:(18)

$$\frac{\Delta H_m}{R} \left(\frac{1}{T_m} - \frac{1}{T} \right) = \ln(v_{\text{drug}}) + \left(1 - \frac{1}{\lambda} \right) (1 - v_{\text{drug}}) + \chi (1 - v_{\text{drug}})^2 \quad (3)$$

where ΔH_m and T_m are the enthalpy of fusion and melting temperature for the pure drug respectively, R is the gas constant, λ is the molar volume ratio of the polymer and drug, χ is the Flory–Huggins interaction parameter. T is the annealing temperature, onset temperature of melting, or dissolution end point temperature, depending on the method in question, and v_{drug} is the volume fraction of drug derived from

$$v_{\text{drug}} = \frac{\frac{X_{\text{drug}}}{\rho_{\text{drug}}}}{\frac{X_{\text{drug}}}{\rho_{\text{drug}}} + \frac{1 - X_{\text{drug}}}{\rho_{\text{polymer}}}} \quad (4)$$

where ρ_{drug} and ρ_{polymer} are the densities of drug and polymer, respectively, and X_{drug} is the mass fraction of drug.

Statistical Analysis

The aim of the statistical analysis was to provide a prediction of the drug–polymer solubility at storage temperature (25 °C). As measurements at such low temperatures are infeasible (or even impossible), one has to rely on extrapolations of data obtained at elevated temperatures from the Flory–Huggins model.(18) The predictions of the drug solubility at room temperature were reported as a central estimate (the least-squares estimate) and a 95% prediction interval in the present study. The predicted solubility was derived from eqs 3 and 4 by inserting the $1 - \alpha$ prediction interval for a future observation of χ given by

$$\hat{\chi} \pm t_{\alpha/2, N-1} s_{\hat{\chi}} \sqrt{1 + \frac{1}{N}} \quad (5)$$

where $\hat{\chi}$ is the least-squares estimate of the interaction parameter, $s_{\hat{\chi}}$ is the standard deviation of $\hat{\chi}$, and $t_{\alpha/2, N-1}$ is the $\alpha/2$ quantile in the t -distribution with $N - 1$ degrees of freedom.

In order to make a proper statistical analysis it is important to realize which variable is subject to experimental noise.

The Recrystallization Method

In the recrystallization method, v_{drug} was subject to error as it was derived from the glass transition temperature of the annealed material. However, as v_{drug} cannot be expressed analytically by rearranging the Flory–Huggins model, the statistical analysis was characterized as an implicit regression problem. The least-squares estimate $\hat{\chi}$ was found by minimizing the residual sum-of-squares given by $SSR(\chi) = \sum_{i=1}^N (v_{\text{drug}}^{\text{measurement}}(i) - v_{\text{drug}}^{\text{fit}}(i; \chi))^2$, where N is the number of measurements. Due to the implicit nature of the problem, the implementation of the analysis requires numerical software, such as MatLab from MathWorks (Natick, MA, USA), which was used in the current work. The standard deviation of χ is given by $s_{\hat{\chi}} = \{SSR(\hat{\chi})/[J^T(\hat{\chi})J(\hat{\chi})]\}^{1/2}$, where $J(\hat{\chi})$ is the Jacobian matrix at $\hat{\chi}$ which was directly obtainable from the nonlinear least-squares routine in MatLab.

The Dissolution End Point Method and the Melting Point Depression Method

For the dissolution end point and melting point depression methods, the experimentally uncertain variable was the melting point, and therefore, the regression problem can be formulated explicitly. The residual sums-of-squares were, for these two methods, given by $SSR(\chi) = \sum_{i=1}^N (\mathcal{T}^{\text{measurement}}(i) - \mathcal{T}^{\text{fitted}}(i; \chi))^2$, where N is the number of measurements. However, it was observed that when the dependent variable was the melting point, the leverage of the fitted values $h_{ii} = \partial \mathcal{T}^{\text{fitted}}(i) / \partial \mathcal{T}^{\text{measurement}}(i)$ was highly variable. Points with high leverages have a larger influence on the fit, which was undesirable as all data points should contribute equally. In order to correct for this, the residual sum-of-squares was studentized: $SSR(\chi) = \sum_{i=1}^N [1/(1 - h_{ii})^{1/2}] [\mathcal{T}^{\text{measurement}}(i) - \mathcal{T}^{\text{fitted}}(i; \chi)]^2$. Due to the simpler structure of the regression problem for these two experimental methods, most software will be able to calculate studentized residuals and the standard deviation of $\hat{\chi}$ directly. For consistency, however, MatLab was also used for this regression problem.

Outlier Detection

Data points that did not follow the pattern described by the Flory–Huggins model can be described as outliers. Removal of outliers from the sample can improve the power of the predictions radically. Therefore, outlier detection was done by calculating Cook's distance of the data points.⁽³¹⁾ Points with Cook's distance larger than three times the mean Cook's distance were removed from the

particular sample analysis. Upon removal, the model was refitted on the new outlier-reduced sample and the Cook's distance was recalculated. This procedure was iterated until no outliers were detected.

Results and Discussion

Liquid Analogue Solubility Approach

The drug–polymer solubility can be estimated from the drug solubility in a liquid low molecular weight analogue using the Flory–Huggins lattice model by assuming that the analogue constitutes the lattice of a polymer and that the interactions and combinatorial entropy of mixing in the drug–analogue and drug–polymer systems are similar.(13, 25)

In this study NVP and VA were used as the analogues because they are the monomeric precursors of the PVP/VA copolymer investigated in this study and structurally identical with the repeat units after polymerization. The solubility of the different drugs in NVP and VA was obtained experimentally from HPLC analysis as described above, and the thermodynamic values used to calculate the activity coefficient in the analogues and polymers were obtained from DSC analysis. The solubility of the five different drugs in the respective PVP/VA copolymers was calculated from the solubility in the liquid NVP and VA monomers and the thermodynamic values given in Table 1 using eqs 1 and 2. The results are given in Table 2.

Table 1. Experimental Physical and Thermodynamic Values of the Materials Measured by DSC and Density Measured by Helium Pycnometry

| material | M_w (g·mol ⁻¹) ^b | density (g·cm ⁻³) ^c | T_g (°C) | ΔC_p (J·g ⁻¹ ·K ⁻¹) | ΔH_m (J·g ⁻¹) |
|------------|---|--|-------------|--|-----------------------------------|
| PCM | 151.17 | 1.22 ± 0.01 | 23.3 ± 0.2 | 0.64 ± 0.04 | 193.5 ± 1.7 |
| CAP | 323.13 | 1.47 ± 0.00 | 29.5 ± 0.3 | 0.54 ± 0.02 | 115.1 ± 0.3 |
| CCX | 381.37 | 1.35 ± 0.01 | 56.8 ± 0.0 | 0.38 ± 0.02 | 99.4 ± 0.8 |
| IMC | 357.79 | 1.31 ± 0.01 | 45.4 ± 0.1 | 0.39 ± 0.01 | 116.7 ± 0.4 |
| FDP | 384.26 | 1.29 ± 0.00 | 45.2 ± 0.1 | 0.36 ± 0.01 | 82.6 ± 0.4 |
| VA | 86.09 | 0.93 ± 0.00 | | | |
| NVP | 111.14 | 1.04 ± 0.00 | | | |
| PVP/VA 335 | 28 000 | 1.18 ± 0.00 | 68.5 ± 0.3 | 0.34 ± 0.01 | |
| PVP/VA 535 | 36 700 | 1.19 ± 0.01 | 91.3 ± 0.1 | 0.34 ± 0.02 | |
| PVP/VA 635 | 38 200 | 1.18 ± 0.01 | 105.3 ± 0.2 | 0.33 ± 0.02 | |
| PVP/VA 735 | 56 700 | 1.18 ± 0.01 | 117.2 ± 0.1 | 0.33 ± 0.02 | |
| PVP K17 | 10 000 | 1.20 ± 0.00 | 125.2 ± 0.4 | 0.31 ± 0.01 | |

^aValues are mean ± SD, $n = 3$. ^bAverage M_w according to the supplier. ^cAmorphous density measured by helium pycnometry.

Table 2. Solubility of the Drugs in NVP and VA and Predicted Solubilities in the Pure Polymers and the Five Drug–Copolymer Systems

| | PCM:PVP/VA 335 | CAP:PVP/VA 535 | CCX:PVP/VA 635 | IMC:PVP/VA 735 | FDP:PVP K17 |
|---|----------------|----------------|----------------|----------------|-------------|
| solubility in NVP at 25 °C (w/w) | 0.34 | 0.71 | 0.61 | 0.52 | 0.12 |
| predicted solubility in PVP at 25 °C (w/w) | 0.18 | 0.52 | 0.41 | 0.31 | 0.05 |
| solubility in VA at 25 °C (w/w) | 0.00 | 0.01 | 0.09 | 0.01 | 0.09 |
| predicted solubility in PVAc at 25 °C (w/w) | 0.00 | 0.00 | 0.03 | 0.01 | 0.04 |
| NVP/VA ratio (w/w) ^a | 30/70 | 50/50 | 60/40 | 70/30 | 100/0 |
| predicted solubility in PVP/VA copolymer at 25 °C (w/w) | 0.05 | 0.26 | 0.26 | 0.22 | 0.05 |

^aWeight ratios according to supplier information.

The solubility (w/w) ranged from 0.00 for PCM in VA to 0.71 for CAP in NVP, and the solubility for all the different drugs was higher in NVP than in VA. After correcting for the reduced entropy of mixing, the predicted solubilities in the pure homopolymers (PVP and PVAc) were reduced drastically compared to those in the analogues. In order to predict the solubility in the copolymer, the solubility in each of the two homopolymers was determined and multiplied by the weight fraction in the copolymer.

The influence of molecular weight on the predicted solubility is negligible for high molecular weight polymers as the term that compensates for molecular weight in eq 2, $1/m_{\text{polymer}}$, approaches zero.(25) Therefore, the solubility of the drugs in the copolymers can be compared without accounting for the difference in molecular weight of the copolymers.

It is important to note that this approach provides an estimate of the solubility in the liquid state rather than in the solid glass and, therefore, should be evaluated with caution.(13) Nevertheless, this approach might still provide valuable indications on the solubility of a drug in a polymer if a liquid analogue of the polymer is available.(29) A review of the Sigma-Aldrich (St. Louis, MO, USA) product range revealed that, in addition to PVP and PVAc, liquid analogues of pharmaceutically relevant polymers are available for polymethacrylates (Eudragit), poly(vinyl alcohol) (PVA), poly(acrylic acid) (Carbomer), polyethylene glycol (PEG), and poly(ethylene oxide) (PEO), but not for cellulose ethers (e.g., hydroxypropylmethylcellulose, HPMC) and polysaccharides (e.g., chitosan).

Recrystallization Method

Thermodynamically, the equilibrium solubility can be measured in at least four different ways, of which the shake-flask method (applied in the liquid analogue solubility approach) is probably the most commonly used. Here the increase of solution concentration is measured from an undersaturated solution at constant temperature.(7) However, this method is impracticable for solid drug–polymer systems due to the solid nature or high viscosity of polymers.

The recrystallization method approaches the equilibrium in a different but thermodynamically equal way, by measuring the *decrease* of solution concentration from a supersaturated solution at constant temperature. As this method relies on the recrystallization of the supersaturated drug from the polymer matrix, it is only feasible to determine the equilibrium solubility above the recrystallization temperature of the supersaturated system.(14) This is because reaching the equilibrium becomes increasingly more time-consuming at temperatures close to the recrystallization temperature due to decreased molecular mobility, which inhibits nucleation and crystallization.(28)

Parameters including drug solubility, polymer T_g and viscosity, degree of supersaturation, and annealing temperature as well as time affect the nucleation and crystallization rate of drugs in supersaturated amorphous solid dispersions. Therefore, it is important to evaluate the drug–polymer

ratio and annealing time/temperatures every time a new drug–polymer system is investigated.(28) Finding the right drug–polymer ratio is a balance between having a too unstable system that recrystallizes before the annealing temperature is reached and a too stable system that will not recrystallize during annealing. The annealing time can be established by monitoring the exothermic recrystallization event during the annealing step, and the process is considered to be in equilibrium after the signal reaches a baseline. However, as the crystallization rate decreases rapidly when the concentration approaches equilibrium solubility,(9) the true equilibrium may not be reached. Nevertheless, in this study, a 3 h annealing time and 80:20 w/w ratios of drug–polymer were found to be suitable for the PCM, CAP, CCX, and FDP systems and 85:15 w/w for the IMC system.

In the original method proposed by Mahieu et al.,(14) the equilibrium solubility concentration after annealing is derived from the T_g of the annealed material using the Gordon–Taylor relationship. However, in this study the composition dependence of the T_g did not correlate with the Gordon–Taylor relationship (data not shown), and therefore, this could not be used to determine the equilibrium solubility after annealing. As an alternative, the experimental composition dependence of the T_g in all systems was used to derive the equilibrium solubility concentration after annealing. Using the annealing temperature and drug fraction, the interaction parameter χ was determined from eqs 3 and 4. The T_g of the annealed materials and the corresponding equilibrium solubilities of the various drugs in the polymers are listed in Table 3. After annealing, it was confirmed that only one T_g was detectable in DSC thermograms for all systems. It was possible to obtain data at annealing temperatures from 115 to 150 °C. At temperatures below 115 °C the time to reach equilibration exceeded the 3 h of annealing, and above 150 °C the drug concentration was not sufficient to saturate the mixture. As anticipated from the liquid analogue solubility approach, the CAP, CCX, and IMC systems exhibited the lowest degree of recrystallization and the PCM and FDP systems the highest.

Table 3. Summary of Raw Data

| Recrystallization Method | | | | | | | | | | | |
|--------------------------|----------------|------------------|----------------|------------------|----------------|------------------|----------------|------------------|-------------|------------------|--|
| T_a (°C) | PCM:PVP/VA 335 | | CAP:PVP/VA 535 | | CCX:PVP/VA 635 | | IMC:PVP/VA 735 | | FDP:PVP K17 | | |
| | T_g (°C) | X_{drug} (w/w) | T_g (°C) | X_{drug} (w/w) | T_g (°C) | X_{drug} (w/w) | T_g (°C) | X_{drug} (w/w) | T_g (°C) | X_{drug} (w/w) | |
| 150 | | | | | 72.0 ± 0.2 | 0.779 | 56.2 ± 0.1 | 0.834 | | | |
| 145 | | | | | 74.3 ± 0.1 | 0.744 | 60.2 ± 0.4 | 0.765 | | | |
| 140 | | | | | 76.5 ± 0.2 | 0.710 | 62.3 ± 0.7 | 0.726 | | | |
| 135 | 45.6 ± 0.3 | 0.414 | 40.2 ± 0.3 | 0.772 | 78.0 ± 0.3 | 0.688 | 64.1 ± 0.7 | 0.693 | 55.5 ± 0.4 | 0.743 | |
| 130 | 47.2 ± 0.1 | 0.385 | 44.8 ± 0.2 | 0.709 | 79.4 ± 0.1 | 0.666 | 65.5 ± 0.5 | 0.667 | 63.6 ± 0.2 | 0.644 | |
| 125 | 48.0 ± 0.1 | 0.370 | 48.4 ± 0.5 | 0.660 | | | 67.2 ± 0.9 | 0.634 | 67.1 ± 0.1 | 0.601 | |
| 120 | 49.4 ± 0.5 | 0.343 | 51.4 ± 0.5 | 0.619 | | | | | 70.2 ± 0.3 | 0.563 | |
| 115 | | | 53.1 ± 0.1 | 0.595 | | | | | | | |

| Dissolution End Point Method | | | | | | | | | | |
|------------------------------|----------------|--|---------------------------|--|--------------------------|--|---------------------------|--|--------------------------|--|
| X_{drug} (w/w) | PCM:PVP/VA 335 | | CAP:PVP/VA 535 | | CCX:PVP/VA 635 | | IMC:PVP/VA 735 | | FDP:PVP K17 | |
| | T_{end} (°C) | | T_{end} (°C) | | T_{end} (°C) | | T_{end} (°C) | | T_{end} (°C) | |
| 0.95 | 172.0 ± 0.04 | | 151.2 ± 0.03 ^b | | 163.8 ± 0.3 ^b | | 161.8 ± 0.02 ^b | | 141.5 ± 0.2 ^b | |
| 0.90 | 171.5 ± 0.3 | | 150.5 ± 0.1 | | 162.8 ± 0.8 | | 160.8 ± 0.02 | | 140.5 ± 0.3 | |
| 0.85 | 169.7 ± 0.03 | | 149.1 ± 0.1 | | 161.1 ± 0.8 | | 159.4 ± 0.1 | | 139.2 ± 0.1 | |
| 0.80 | 168.8 ± 0.1 | | 146.7 ± 0.1 | | 158.3 ± 0.6 | | 156.9 ± 0.1 | | 137.3 ± 0.2 | |
| 0.75 | 168.6 ± 0.4 | | 143.9 ± 0.04 | | 154.5 ± 0.6 | | 152.3 ± 0.2 | | 134.9 ± 0.2 | |
| 0.70 | 167.4 ± 0.3 | | 140.2 ± 0.5 | | 150.1 ± 0.3 | | 147.3 ± 0.3 | | 132.0 ± 0.1 | |
| 0.65 | 165.1 ± 0.6 | | | | 148.3 ± 0.2 ^b | | 140.5 ± 1.2 | | | |
| 0.60 | 163.5 ± 0.6 | | | | | | 132.4 ± 1.0 | | | |

| Melting Point Depression Method | | | | | | | | | | |
|---------------------------------|----------------|--|----------------|--|----------------|--|----------------|--|--------------------------|--|
| X_{drug} (w/w) | PCM:PVP/VA 335 | | CAP:PVP/VA 535 | | CCX:PVP/VA 635 | | IMC:PVP/VA 735 | | FDP:PVP K17 | |
| | T_m (°C) | | T_m (°C) | | T_m (°C) | | T_m (°C) | | T_m (°C) | |
| 0.95 | 168.5 ± 0.01 | | 148.4 ± 0.1 | | 160.1 ± 0.04 | | 158.3 ± 0.1 | | 140.8 ± 0.1 ^b | |
| 0.90 | 167.5 ± 0.2 | | 145.9 ± 0.1 | | 157.6 ± 0.03 | | 154.8 ± 0.1 | | 139.9 ± 0.02 | |
| 0.85 | 166.4 ± 0.3 | | 141.9 ± 0.4 | | 152.2 ± 0.4 | | 145.0 ± 0.3 | | 138.6 ± 0.01 | |
| 0.80 | 164.8 ± 0.3 | | 139.2 ± 0.3 | | 145.5 ± 0.2 | | 144.6 ± 0.1 | | 138.1 ± 0.01 | |
| 0.75 | 159.8 ± 0.5 | | | | | | | | | |
| 0.70 | 156.1 ± 0.3 | | | | | | | | 137.3 ± 0.3 | |
| 0.65 | 151.1 ± 0.1 | | | | | | | | | |
| 0.60 | 142.5 ± 0.1 | | | | | | | | 136.9 ± 0.01 | |

A For the recrystallization method, the glass transition temperatures of the annealed material (T_g) and the corresponding drug fraction (X_{drug}) were measured at different annealing temperatures (T_a). For the dissolution end point and melting point depression methods, the dissolution end point (T_{end}) and melting point (T_m) were measured at different drug fractions (X_{drug}) (values are mean ± SD, $n = 3$).

B Data detected as outlier by calculation of Cook's distance and excluded.(31)

Dissolution End Point and Melting Point Depression Methods

As described in the Introduction, it is possible to relate the magnitude of melting point depression (chemical potential reduction) to the solubility of a drug–polymer system using the Flory–Huggins model.(18, 19)

Pure crystalline materials melt at a temperature when the chemical potential of the crystalline and liquid states is equal. If an “impurity”, such as a polymer, is added to the crystalline material, the chemical potential can be reduced compared to that of the pure crystalline material.(18) This reduction in chemical potential can be observed using DSC through detection of a depressed melting point.(11, 12) For drug–polymer systems this phenomenon is observed when the dissolution of the

crystalline drug into the amorphous polymer is favored by the thermodynamics of mixing due to solid state interactions between the drug and polymer.(12) Consequently, it is expected that the depression of the melting point is greater if mixing is exothermic compared to athermal or endothermic mixing and not present for immiscible systems.(13)

The level of mixing of the components as well as the particle size will affect the accuracy of the DSC measurements as the dissolution requires transport of molecules into the polymer matrix. If the components are poorly mixed and contain large particles, mixing requires transport over long distances, which will result in a thermal lag. This can be accounted for by decreasing the heating rate or introducing milling of the sample to reduce the particle size and increase the level of mixing. Intensive low-temperature milling of physical mixtures can increase the drug–polymer surface interactions and reduce diffusive mixing to a point where dissolution of the crystalline drug is completed during the thermal analysis; however, milling is also known to potentially render the drug (partially) amorphous.(32) Consequently, for the dissolution end point method, a degree of amorphization is promoted, but complete amorphization should be avoided. In contrast, for the melting point depression method, as the drug–polymer solubility is derived from the chemical potential difference in the Flory–Huggins model, it is important that the drug fraction be 100% crystalline.

The determination of the melting point of the crystalline drug represents the ideal case assuming that it can be obtained in an equilibrium transition state.(21) Therefore, the melting point is ideally recorded at zero heating rate;(11) however, as this is not possible in practice, the heating rate should be slow enough to induce molecular mixing. Conversely, from a practical point of view, it is also desirable to reduce the duration of the DSC run, and thus, the optimal heating rate depends on the molecular mobility of the system and, hence, the viscosity and T_g of the polymer. If the T_g of the polymer is above the temperature of equilibrium, the molecular mobility in the polymer might be so low that mixing of the components becomes slower than the time scale of the DSC measurement.(11) Therefore, the application of these methods to predict drug–polymer solubility is limited to polymers with a relatively low T_g . In this study, data was only recorded at temperatures above the T_g of the polymer, and a heating rate of 1 °C/min was applied as this rate was believed to be sufficiently low to induce molecular mixing while providing data relatively fast.

Finally, it is still debated whether to use the onset or end point values of melting to determine the Flory–Huggins interaction parameter. While both methods are still being applied, the end point is currently most commonly used to determine the solubility of drugs in polymers in the literature.(10, 11, 13, 24, 25, 27) The underlying argument is that this value represents the melting point of the final composition, assuming that complete mixing has occurred.(11, 13, 23) Nevertheless, more research is

needed in order to ultimately determine what the most appropriate method is. Therefore, in this study both the onset and end point values were obtained from the two different methods and compared. The data obtained from the two different methods can be found in Table 3, and the interaction parameter χ from the dissolution end point and melting point depression was derived directly from the data by applying eqs 3 and 4. From Table 3 it can be seen that both methods demonstrated some degree of melting point depression, suggesting that all systems were miscible. As expected, the onset values were lower than the end point values using the two different methods. However, for the FDP:PVP K17 system the onset values were higher than the end point values, indicating a discrepancy. As both methods use the same heating rate, this discrepancy could be due to the intimate milling (and perhaps partial amorphization) applied in the dissolution end point method.

Comparison of the Different Methods

The predicted solubility at 25 °C of the five drug–copolymer systems using the four different methods can be found in Figure 1 and Table 4 along with χ values and 95% prediction intervals. Note that the estimates from the liquid analogue solubility approach do not include a 95% prediction interval. This is because the estimates were based on a single-point determination obtained at 25 °C and thus not obtained from extrapolation. Representative equilibrium solubility curves of the IMC:PVP/VA 735 system using the data obtained from the three different thermal analysis methods are shown in Figure 2. As the value of χ is influenced by all factors in the Flory–Huggins model, it is not comparable between the different systems or methods. Therefore, the evolution of the solubility curve or the predicted solubility at 25 °C rather than χ should be used for comparison. The predicted solubilities at 25 °C vary considerably depending on whether (dissolution) end point or (melting point depression) onset values are used. Defining which of the methods is better requires more effort to understand the difference in detail and is beyond the scope of the current work; however, this is certainly something which should be considered when selecting experimental method.

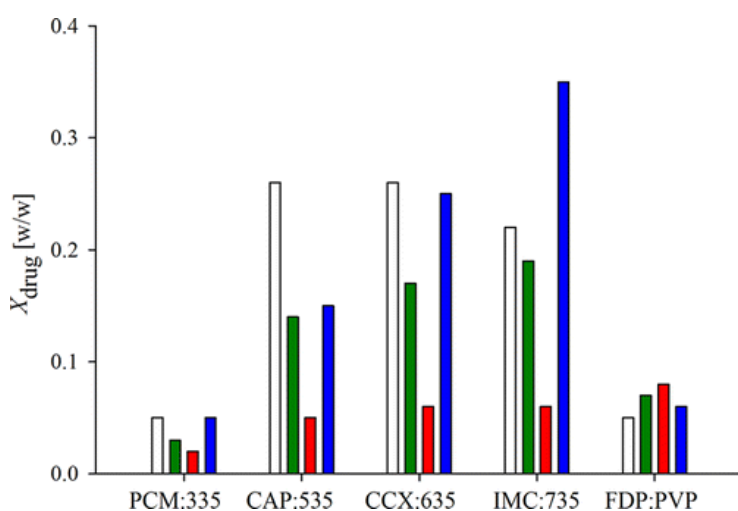


Figure 1. Graphical illustration of the drug–polymer solubilities of the five systems predicted from the four different methods presented in Table 4. The white bars represent the liquid analogue solubility approach, the green bars represent the recrystallization method, the red bars represent the dissolution end point method, and the blue bars represent the melting point depression method.

Table 4. Drug–Polymer Solubilities of the Five Systems Predicted from the Four Different Methods along with the Flory–Huggins Interaction Parameter χ and the 95% Prediction Interval

| | PCM:PVP/VA 335 | CAP:PVP/VA 535 | CCX:PVP/VA 635 | IMC:PVP/VA 735 | FDP:PVP K17 |
|----------------------------------|--|----------------|----------------|----------------|----------------|
| | Liquid Analogue Solubility Approach | | | | |
| solubility at 25 °C (w/w) | 0.05 | 0.26 | 0.26 | 0.22 | 0.05 |
| | Recrystallization Method | | | | |
| interaction parameter χ | -1.2 ± 0.3 | -4.1 ± 1.0 | -5.2 ± 0.9 | -6.3 ± 1.6 | -2.2 ± 0.6 |
| solubility at 25 °C (w/w) | 0.03 | 0.14 | 0.17 | 0.19 | 0.07 |
| 95% prediction interval at 25 °C | 0.02–0.04 | 0.08–0.20 | 0.12–0.21 | 0.11–0.25 | 0.04–0.10 |
| | Dissolution End Point Method | | | | |
| interaction parameter χ | -0.6 ± 0.9 | -1.9 ± 0.8 | -2.9 ± 1.6 | -2.9 ± 0.9 | -1.4 ± 0.6 |
| solubility at 25 °C (w/w) | 0.02 | 0.05 | 0.06 | 0.06 | 0.08 |
| 95% prediction interval at 25 °C | 0.01–0.04 | 0.03–0.09 | 0.01–0.14 | 0.03–0.10 | 0.05–0.12 |
| | Melting Point Depression Method | | | | |
| interaction parameter χ | -1.3 ± 0.8 | -3.9 ± 1.8 | -5.7 ± 1.1 | -8.8 ± 3.7 | -1.5 ± 3.0 |
| solubility at 25 °C (w/w) | 0.05 | 0.15 | 0.25 | 0.35 | 0.06 |
| 95% prediction interval at 25 °C | 0.02–0.09 | 0.05–0.26 | 0.19–0.31 | 0.18–0.45 | 0.00–0.25 |

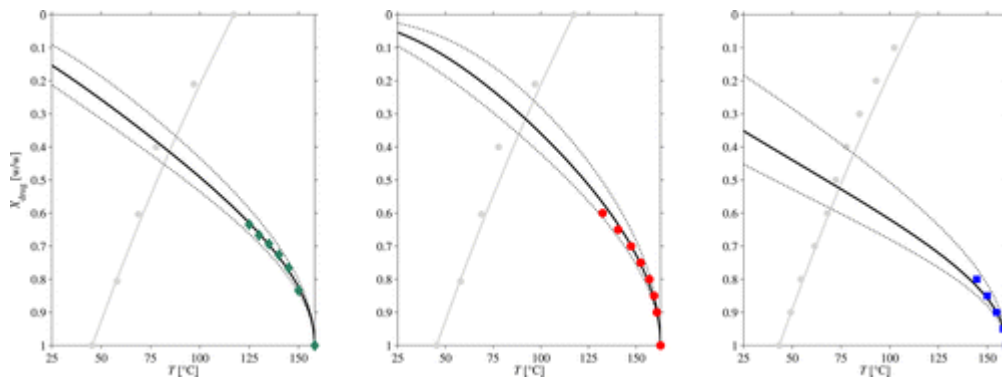


Figure 2. Representative equilibrium solubility curves of IMC (X_{drug}) in PVP/VA 735 as a function of temperature (T) from the three different thermal analysis methods. Green diamonds (\blacklozenge) represent the data from the recrystallization method, red circles (\bullet) represent the data from the dissolution end point method, and blue squares (\blacksquare) represent the data from the melting point depression method. All data points are illustrated as averages ($n = 3$). The evolution of solubility of the three data sets has been fitted with the Flory–Huggins model (black curves) including the 95% prediction interval (dotted curves). The gray circles (\bullet) represent the experimental relationship between T_g and X_{drug} , and the gray curve is the theoretical Gordon–Taylor relationship.

From Figure 1 and Table 4 it is evident that the recrystallization and melting point depression methods rank the predicted solubility in the same order, IMC-PVP/VA 735 > CCX-PVP/VA 635 > CAP-PVP/VA 535 > FDP-PVP K17 > PCM–PVP/VA 335. Except for the FDP-PVP K17 system, this ranking is identical to the predicted solubility obtained from the dissolution end point method, but different from that

predicted by the liquid analogue solubility approach. However, the magnitude of the predicted solubilities from the recrystallization method and melting point depression method correlated well with the predictions from the liquid analogue solubility approach. This suggests that this method can be used to screen for drug solubility in polymers if a liquid analogue is available.

The solubility predictions at 25 °C based on the recrystallization method were consistently higher than the predictions based on dissolution end point method (except for FDP-PVP K17). This difference was to some extent expected, as the thermodynamics behind the two methods are fundamentally different. The recrystallization method approaches equilibrium solubility from the supersaturated state, and the equilibrium thermodynamics are driven by recrystallization kinetics. In contrast, the dissolution end point method approaches equilibrium solubility from an undersaturated state and the equilibrium thermodynamics are thus driven by dissolution kinetics.

In addition to being dependent on temperature and viscosity,(25) the recrystallization and dissolution kinetics slow down when the concentration approaches equilibrium solubility. In fact, the recrystallization kinetics may be so slow that it is not detectable in the DSC and, therefore, the system can falsely be considered in equilibrium.(28) This could give a reason to believe that the recrystallization method might be overestimating the solubility. Furthermore, as the dissolution end point method relies on dissolution kinetics that are expected to be slower than recrystallization kinetics,(14) an underestimation of the solubility is expected. It is therefore rational to assume that the true solubility is somewhere between that predicted by the recrystallization and dissolution end point methods. Even though this is a hypothesis left unverified in this study, it could explain why the predicted solubility was consistently higher when using the recrystallization method compared to the dissolution end point method.

A way of limiting the prediction error is to increase the annealing time and lower the heating rate to allow for equilibrium to be reached for the recrystallization method and dissolution end point method, respectively. However, due to the previously mentioned slow kinetics, this would drastically increase the duration of the experiments and probably not impact the solubility prediction significantly.

In the case of the melting point depression method, the evaluation of the prediction is more complex. As the method is not based on equilibrium thermodynamics, it is difficult to say whether the method is under- or overestimating the solubility. However, this could be investigated by annealing the sample at the determined T_m until equilibrium has been reached and subsequent scanning for a residual dissolution endotherm, as proposed by Sun et al.(7) The presence of a dissolution endotherm after annealing indicates that the dissolution is not completed and that the "true" T_m is located above the annealing temperature. This approach is very time-consuming and is therefore laborious compared to the methods used in this study. Due to the nature of the method and as the solubility data from the

melting point depression method was not significantly different from that of the recrystallization method, it is expected that the melting point depression method is also likely to overestimate solubility. The advantages and disadvantages of the four different methods are summarized in Table 5.

Table 5. Advantages and Disadvantages of the Four Different Methods

| advantages | disadvantages |
|---|---|
| Liquid Analogue Solubility Approach | |
| simple shake-flask method | requires liquid analogue |
| measures at room temperature | predicts the solubility in a liquid rather than a solid |
| enables multiple screening | |
| Recrystallization Method | |
| heating rate independent | time-consuming |
| applicable for most polymers with $T_g > 90\text{ }^\circ\text{C}^a$ | may overestimate solubility |
| Dissolution End Point Method | |
| applicable for most polymers with $T_g < 120\text{ }^\circ\text{C}^a$ | heating rate and milling condition dependent |
| relatively fast | may underestimate solubility |
| | not applicable if drug is thermally decomposed at T_m |
| Melting Point Depression Method | |
| applicable for most polymers with $T_g < 120\text{ }^\circ\text{C}^a$ | heating rate dependent |
| relatively fast | may overestimate solubility |
| | requires 100% crystallinity |
| | not applicable if drug is thermally decomposed at T_m |

A Estimation based on a general assumption of the T_m ($>140\text{ }^\circ\text{C}$) and T_g ($<70\text{ }^\circ\text{C}$) of low molecular weight drugs.(36)

The negative χ value, signifying miscibility predicted for all systems in this study, is, to some extent, also supported by the experimental deviation from the theoretical Gordon–Taylor relationship as mentioned previously (data not shown). The Gordon–Taylor relationship is based on ideal mixing behavior (additivity) of the two components. Deviations from the ideal behavior are the result of entropy effects beyond combinatorial mixing such as strong intermolecular interactions.(33) As cohesive intermolecular interactions (e.g., hydrogen bonds) favor miscibility,(12) it is rational to assume that strong/numerous interactions indicate good miscibility between the components.

As can be derived from the data presented in Table 4, the predictions based on the recrystallization method were more precise (relatively) than the predictions based on the melting point depression and dissolution end point methods. This is probably a result of the nature of these methods as the interaction parameter is more sensitive to experimental uncertainty, at temperatures closer to the

melting point of the pure drug. Even a small change in the melting temperature will have a large impact on χ and thus also the curve fitting and predicted solubility at 25 °C. Therefore, it is recommended that data points are only obtained for compositions lower than 90% drug. Conversely, at lower drug contents the dissolution kinetics can potentially exceed the time scale of the experiment depending on heating rate. In order to account for thermal lag and the influence of the heating rate on the phase equilibrium temperature, Tao et al.(11) proposed an extrapolation of the temperature to zero heating rate. However, the validity and linearity of these extrapolations has still not been confirmed. Generally for a glass solution to be pharmaceutically relevant, the drug–polymer solubility should ideally be higher than 20% w/w at typical storage temperatures.(34) Consequently, based on the findings of this study, a decision tree for the screening of polymers suitable for glass solutions has been proposed in Figure 3. It is important to emphasize that the decision tree is designed for the selection of polymers suitable for glass solutions only and thus do not regard considerations of kinetic stability. This means that polymers classified as unsuitable for glass solutions according to the decision tree are not necessarily also unsuitable for (kinetically stabilized) solid dispersions.

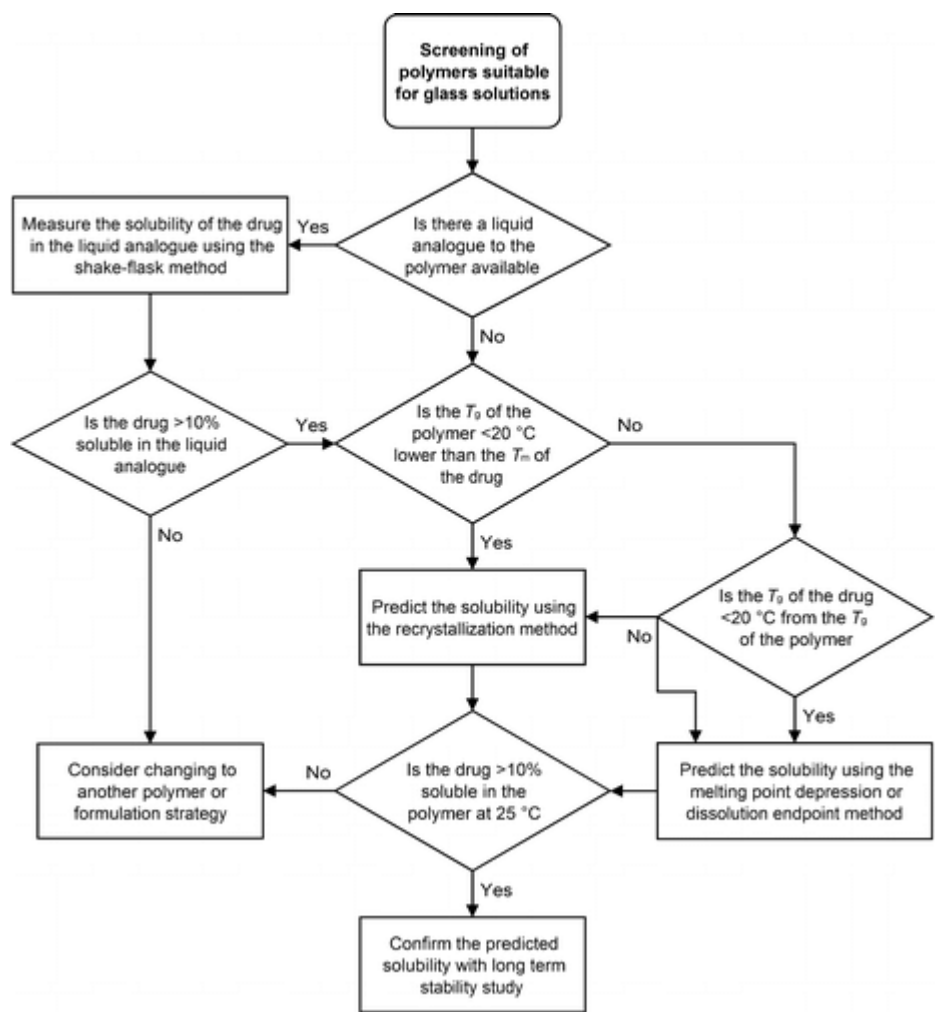


Figure 3. Decision tree for the screening of polymers suitable for glass solutions including the selection of the most optimal methods to predict drug–polymer solubility. Please note that this does not regard considerations of kinetic stability.

The proximity of the Hildebrand solubility parameter of the drug to that of the copolymer ($\pm 7.5 \text{ MPa}^{1/2}$) has been proposed to indicate miscibility between the compounds.⁽³⁵⁾ This could potentially give valuable indications on the drug–polymer solubility and speed up the screening process (by excluding unpromising polymers early in the screening). However, no direct correlation between the proximity of the Hildebrand solubility parameter and drug–polymer or drug–analogue solubility was found in this study (data not shown). Therefore, it is recommended that the screening be initiated by determining the solubility in liquid analogues of pharmaceutically relevant polymers if available. If the drug is not freely soluble (<10% w/w) in an analogue of the polymer, it is most likely also not soluble in the polymer, and therefore, a change to a structurally different polymer should be considered. Having established the most promising polymer candidates from the liquid analogue solubility approach, the solubility of the drug in the polymers can now be predicted from one or more of the three thermal analysis methods. Which of these three different thermal analysis methods are optimal for the prediction of drug–polymer solubility is dependent on the thermal properties of both the drug and polymer. If the T_g of the polymer is higher than the T_m of the drug or the difference between the T_m of the drug and T_g of the polymer is less than 20 °C, the mixing of the components might be slower than the time scale of the DSC measurement and, therefore, the recrystallization method should be used. On the other hand, if the difference between T_g of the polymer and the T_g of the drug is less than 20 °C, the experimental composition dependence of the T_g might not be sufficient to derive the equilibrium solubility concentration with satisfactory precision after annealing. In this case, it is recommended that drug–polymer solubility be predicted from the dissolution end point or melting point depression method. If none of the above restrictions apply, all three thermal analysis methods can be used to predict the drug–polymer solubility. As mentioned previously an overestimation of the solubility should be expected when using the recrystallization and melting point depression methods and an underestimation should be expected when using the dissolution end point method. The data obtained at elevated temperature from the thermal analysis method(s) is then fitted with the Flory–Huggins model and extrapolated in order to predict the solubility at ambient temperature. If the drug is not freely soluble (>10% w/w) in the polymer, then a change to another polymer or formulation strategy should be considered. Finally, for the most promising polymer(s), the drug–polymer solubility can be confirmed with long-term stability at dry conditions at room temperature.

Conclusions

In this work, a comparative study of different methods to predict drug–polymer solubility was carried out. The drug–polymer solubility at 25 °C was predicted by extrapolation of data obtained at elevated temperature using the Flory–Huggins model. The predictions from the recrystallization and melting point depression methods provided similar predictions that were consistently higher than the predictions made from the dissolution end point method. Furthermore, the recrystallization method provided smaller confidence intervals of the predictions (relatively) compared to the dissolution end point and melting point depression methods due to a better fit of the obtained data to the Flory–Huggins model. All methods could successfully produce data with satisfactory reproducibility that fitted relatively well with the Flory–Huggins model, and thus, no limitations to the methods were discovered. The learnings of this comparative study provided a general guidance for the selection of the most suitable thermal analysis method for the screening of drug–polymer solubility. However, defining which of the thermal analysis methods is superior requires more effort to understand in detail and will have to be investigated in future work.

The authors declare no competing financial interest.

Acknowledgment

The authors would like to thank E. B. Jørgensen of the Department of Biologics and Pharmaceutical Science at H. Lundbeck A/S for his contribution to the HPLC measurements. This publication has emanated from research supported in part by the Irish Research Council and Eli Lilly S.A. through an Irish Research Council Enterprise Partnership Scholarship for C.M.B., in part by The Royal Society in the form of Industrial Fellowship awarded to G.A., and in part by a research grant from Science Foundation Ireland (SFI) under Grant Number SFI/12/RC/2275 (for A.M.H., L.T., K.P., and A.K.).

References

1. Hancock, B. C.; Zografi, G. Characteristics and significance of the amorphous state in pharmaceutical systems *J. Pharm. Sci.* 1997, 86 (1) 1– 12
2. Leuner, C.; Dressman, J. Improving drug solubility for oral delivery using solid dispersions *Eur. J. Pharm. Biopharm.* 2000, 50 (1) 47– 60
3. Yu, L. Amorphous pharmaceutical solids: preparation, characterization and stabilization *Adv. Drug Delivery Rev.* 2001, 48 (1) 27– 42

4. Serajuddin, A. T. Solid dispersion of poorly water-soluble drugs: early promises, subsequent problems, and recent breakthroughs *J. Pharm. Sci.* 1999, 88 (10) 1058– 1066
5. Craig, D. Q. The mechanisms of drug release from solid dispersions in water-soluble polymers *Int. J. Pharm.* 2002, 231 (2) 131– 144 DOI: 10.1016/S0378-5173(01)00891-2 [Crossref], [PubMed], [CAS]
6. Grohganz, H.; Priemel, P. A.; Lobmann, K.; Nielsen, L. H.; Laitinen, R.; Mullertz, A.; Van den Mooter, G.; Rades, T. Refining stability and dissolution rate of amorphous drug formulations *Expert Opin. Drug Delivery* 2014, 11 (6) 977– 989
7. Sun, Y.; Tao, J.; Zhang, G. G.; Yu, L. Solubilities of crystalline drugs in polymers: an improved analytical method and comparison of solubilities of indomethacin and nifedipine in PVP, PVP/VA, and PVAc *J. Pharm. Sci.* 2010, 99 (9) 4023– 4031
8. Hancock, B. C.; Shamblin, S. L.; Zografi, G. Molecular mobility of amorphous pharmaceutical solids below their glass transition temperatures *Pharm. Res.* 1995, 12 (6) 799– 806
9. Yoshioka, M.; Hancock, B. C.; Zografi, G. Crystallization of indomethacin from the amorphous state below and above its glass transition temperature *J. Pharm. Sci.* 1994, 83 (12) 1700– 1705
10. Tian, Y.; Booth, J.; Meehan, E.; Jones, D. S.; Li, S.; Andrews, G. P. Construction of drug–polymer thermodynamic phase diagrams using Flory–Huggins interaction theory: identifying the relevance of temperature and drug weight fraction to phase separation within solid dispersions *Mol. Pharmaceutics* 2013, 10 (1) 236– 248
11. Tao, J.; Sun, Y.; Zhang, G. G.; Yu, L. Solubility of small-molecule crystals in polymers: D-mannitol in PVP, indomethacin in PVP/VA, and nifedipine in PVP/VA *Pharm. Res.* 2009, 26 (4) 855– 864
12. Marsac, P. J.; Shamblin, S. L.; Taylor, L. S. Theoretical and practical approaches for prediction of drug-polymer miscibility and solubility *Pharm. Res.* 2006, 23 (10) 2417– 2426
13. Marsac, P. J.; Li, T.; Taylor, L. S. Estimation of drug-polymer miscibility and solubility in amorphous solid dispersions using experimentally determined interaction parameters *Pharm. Res.* 2009, 26 (1) 139– 151
14. Mahieu, A.; Willart, J. F.; Dudognon, E.; Danede, F.; Descamps, M. A new protocol to determine the solubility of drugs into polymer matrixes *Mol. Pharmaceutics* 2013, 10 (2) 560– 566

15. Amharar, Y.; Curtin, V.; Gallagher, K. H.; Healy, A. M. Solubility of crystalline organic compounds in high and low molecular weight amorphous matrices above and below the glass transition by zero enthalpy extrapolation *Int. J. Pharm.* 2014, 472 (1–2) 241– 247
16. Mohan, R.; Lorenz, H.; Myerson, A. S. Solubility measurement using differential scanning calorimetry *Ind. Eng. Chem. Res.* 2002, 41 (19) 4854– 4862
17. Xie, X. L.; Li, R. K. Y.; Tjong, S. C.; Tang, C. Y. Flory-huggins interaction parameters of LCP/thermoplastic blends measured by DSC analysis *J. Therm. Anal. Calorim.* 2002, 70 (2) 541– 548
18. Flory, P. J. *Principles of polymer chemistry*; Cornell University Press: Ithica, NY, 1953.
19. Hoesi, Y.; Yamaura, K.; Matsuzawa, S. A lattice treatment of crystalline solvent-amorphous polymer mixtures on melting point depression *J. Phys. Chem.* 1992, 96 (26) 10584– 10586
20. Koningsveld, R.; Stockmayer, W. H.; Nies, E. *Polymer phase diagrams: a textbook*; Oxford University Press: 2001.
21. Zhao, Y.; Inbar, P.; Chokshi, H. P.; Malick, A. W.; Choi, D. S. Prediction of the thermal phase diagram of amorphous solid dispersions by Flory-Huggins theory *J. Pharm. Sci.* 2011, 100 (8) 3196– 3207
22. Lu, J.; Shah, S.; Jo, S.; Majumdar, S.; Gryczke, A.; Kolter, K.; Langley, N.; Repka, M. A. Investigation of phase diagrams and physical stability of drug-polymer solid dispersions *Pharm. Dev. Technol.* 2015, 20 (1) 105– 117
23. Nishi, T.; Wang, T. T. Melting point depression and kinetic effects of cooling on crystallization in poly (vinylidene fluoride)-poly (methyl methacrylate) mixtures *Macromolecules* 1975, 8 (6) 909– 915
24. Lin, D.; Huang, Y. A thermal analysis method to predict the complete phase diagram of drug-polymer solid dispersions *Int. J. Pharm.* 2010, 399 (1) 109– 115
25. Paudel, A.; Van Humbeeck, J.; Van den Mooter, G. Theoretical and experimental investigation on the solid solubility and miscibility of naproxen in poly(vinylpyrrolidone) *Mol. Pharmaceutics* 2010, 7 (4) 1133– 1148

26. Caron, V.; Tajber, L.; Corrigan, O. I.; Healy, A. M. A comparison of spray drying and milling in the production of amorphous dispersions of sulfathiazole/polyvinylpyrrolidone and sulfadimidine/polyvinylpyrrolidone *Mol. Pharmaceutics* 2011, 8 (2) 532– 542
27. Donnelly, C.; Tian, Y.; Potter, C.; Jones, D. S.; Andrews, G. P. Probing the Effects of Experimental Conditions on the Character of Drug-Polymer Phase Diagrams Constructed Using Flory-Huggins Theory *Pharm. Res.* 2015, 32 (1) 167– 179
28. Knopp, M. M.; Olesen, N. E.; Holm, P.; Löbmann, K.; Holm, R.; Langguth, P.; Rades, T. Evaluation of drug-polymer solubility curves through formal statistical analysis: comparison of preparation techniques *J. Pharm. Sci.* 2015, 104 (1) 44– 51
29. Knopp, M. M.; Olesen, N. E.; Holm, P.; Langguth, P.; Holm, R.; Rades, T. Influence of Polymer Molecular Weight on Drug-Polymer Solubility: A Comparison between Experimentally Determined Solubility in PVP and Prediction Derived from Solubility in Monomer *J. Pharm. Sci.* 2015,
30. Gordon, M.; Taylor, J. S. Ideal copolymers and the second-order transitions of synthetic rubbers. i. non-crystalline copolymers *J. Appl. Chem.* 1952, 2 (9) 493– 500
31. Cook, R. D. Detection of influential observation in linear regression *Technometrics* 1977, 19, 15– 18
32. Crowley, K. J.; Zografi, G. The effect of low concentrations of molecularly dispersed poly(vinylpyrrolidone) on indomethacin crystallization from the amorphous state *Pharm. Res.* 2003, 20 (9) 1417– 1422
33. Pinal, R. Entropy of mixing and the glass transition of amorphous mixtures *Entropy* 2008, 10 (3) 207– 223
34. Huang, Y.; Dai, W.-G. Fundamental aspects of solid dispersion technology for poorly soluble drugs *Acta Pharm. Sin. B* 2014, 4 (1) 18– 25
35. Greenhalgh, D. J.; Williams, A. C.; Timmins, P.; York, P. Solubility parameters as predictors of miscibility in solid dispersions *J. Pharm. Sci.* 1999, 88 (11) 1182– 1190
36. Alzghoul, A.; Alhalaweh, A.; Mahlin, D.; Bergstrom, C. A. Experimental and computational prediction of glass transition temperature of drugs *J. Chem. Inf. Model.* 2014, 54 (12) 3396– 3403

